International Journal of Nanotechnology and Applications
ISSN 0973-631X Volume 11, Number 2 (2017), pp. 127-135

http://www.ripublication.com

Magnetic, Optical properties of $Zn_{1-x}Mn_xS$ thin films prepared by Chemical Bath Deposition (CBD) technique

Adel Sadoon[a] and Ramphal Sharma [a, b]

[1]*Department of Nanotechnology, Dr. Babasaheb Ambedkar Marathwada University, Aurangabad*

[2]*Thin film and Nanotechnology Laboratory, Department of Physics Dr. Babasaheb Ambedkar Marathwada University, Aurangabad.*

Abstract

$Zn_{1-x}Mn_xS$ thin films were deposited on glass substrates using a chemical bath deposition (CBD) method in an aqueous solution is an important semiconductor with a wide band gap and high transparency in the UV-visible region . The optical properties of the film were studied using measurement from UV-Vis spectrophotometer; the results appear that an optical absorption edge was blue shifted region and estimated band gap value of ZnS, ZnMnS and MnS was 3.7eV 3.93eV and 3.33eV respectively . Magnetic measurements showed that a paramagnetic behavior at 0 at.% and ferromagnetic behavior at 20 at.% and 100 at.% .

Key words: Nanostructured, CBD, magnetic, $Zn_{1-x}Mn_xS$, doped,.. etc.

1. INTRODUCTION

The II-VI compounds semiconductor thin films (e.g. CdS ,ZnS ,CdSe, ZnSe) have received an intensive attention due to their application in thin film solar cells, optical coatings , optoelectronic devices ,and light emitting diodes [1-2].Among these metal chalcogenids , ZnS is an important semiconductor material because of its broad, direct band gap energy(~3.6eV) at room temperature, high refractive index (2.35), and high dielectric constant. Zinc sulfide is a semiconductor suitable for use as a host matrix for a wide variety of dopants on account of its wide energy band gap. The luminescence properties of this material doped with Mn have proven to be suitable for electroluminescence applications[3-5] .Manganese is generally incorporated as Mn^{2+}

ion in the substitutional sites of the ZnS lattice. The techniques used to deposit ZnS films have different natures. Among them, the most common are sputtering,[6] sol-gel,[3,7] spray pyrolysis,[8,9] chemical vapor deposition (CVD),[10,11] molecular beam epitaxy,[12] atomic layer epitaxy (ALE),[13] and chemical bath deposition (CBD)[14-20]. Among these ,the CBD method is much more attractive since the technique possesses a number of advantages over the conventional thin film deposition methods including the simplicity in experimental set up .It does not require an expensive vacuum system. The main advantages of the CBD method are low cost, low deposition temperature, easy coating of large surfaces, and having the capacity to deposit optically smooth, uniform, and homogeneous layers [21-22].

2 MATERIALS AND METHODS

1.1 Materials

All chemical used in the experiment were analytic reagent grade. Zinc sulphate hepta hydrate $ZnSO_4.6H_2O$, manganese sulphate ($MnSO_4.H_2O$) and Thioacetamide were purchased from Merck chemical (India) Pvt. Ltd. Ammonia and triethaloamine also purchased from Merck chemical (India) Pvt. Ltd, Double deionized water was used through out the experiment.

1.2 Synthesis of nanostructured $Zn_{1-x}Mn_xS$ thin film

Preparation of $Zn_{1-x}Mn_xS$ ($x = 0$, 0.2 and 1) thin films. Nanocrystalline $Zn_{1-x}Mn_xS$ thin films were deposited on commercial microscope slide glass substrates . A very attractive method for producing ZnS thin films due to possibility of large area deposition of sulphides, oxides so called chemical bath deposition method. $Zn_{1-x}Mn_xS$ thin films are prepared by decomposition of triethaloamine in an alkaline solution containing a zinc salt, manganese sult and a suitable complexing agent .The deposition process is based on the release of Zn^{2+}, Mn^{2+} and S^{2-} ions in solution which then condense on the substrate. Before film deposition, the substrates were first cleaned in chromic acid solution and were subsequently washed in detergent solution, rinsed in deionized water. The substrates were then dried in air(The cleaned glass surface provided nucleation centre for growth, good adhesion and uniform deposition of the films). The coated substrates for (x= 0 , 0.2 and 1) were removed at the end of deposition, washed in deionized water, dried in air at room temperature, and then characterized. Both sides of the glass substrates were coated with the films.

2. RESULTS AND DISCUSSIONS

3.1 Optical study of $Zn_{1-x}Mn_xS$ (ZnS) thin film were x=0

The optical absorbance of ZnS thin film is determined from the range 300-900 nm**.**

(Fig 1a) shows absorbance as-deposited nanostructured ZnS thin film.

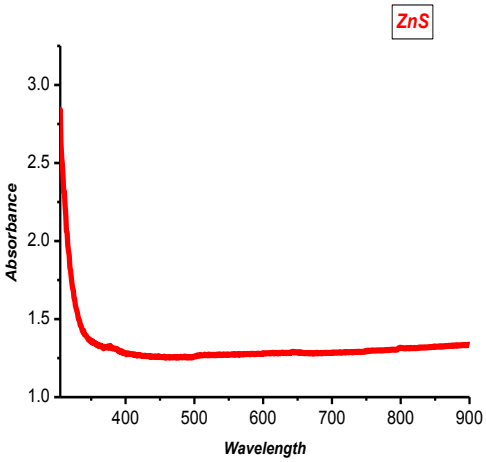

(Fig.1a) Shows absorption spectra of $Zn_{1-x}Mn_xS$ (ZnS) thin film were x=0

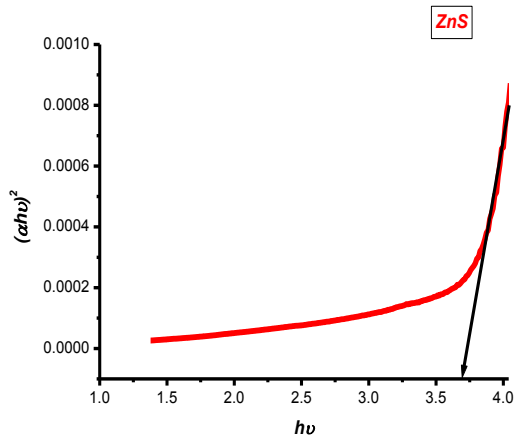

(Fig.1b) shows the band gap of nanostructured ZnS thin film.

(Fig 1b) shows band gap of nanostructured ZnS thin film obtained from absorption spectra. The relation between the absorption coefficient α and the incident photon energy (hν) is given by relation.

$$\alpha = \frac{A\left(h\nu - E_g\right)^n}{h\nu}$$

In this relation n= ½ is taken for direct allowed transition and 'Eg' is optical band material. Absorption coefficient (α) is associated with the strong absorption region of thin films was calculated from absorbance (A). Eg is the separation between the valence and conduction bands and n is a constant that is equal to 1 for direct band gap semiconductors. These band gap values are higher than the bulk value of hexagonal ZnS because of quantum confinement in ZnS nanocrystals. The band gap energy could be obtained from the plot of $(\alpha h \nu)^2$ as a function of $h \nu$ (Figure 1b). A sharp cut off is obtained from absorption spectra at ~303 nm which corresponds to band gap energy of 3.70eV [21,22].

3.2 Optical study of $Zn_{1-x}Mn_xS$ (MnS) thin film were (x=1)

The optical absorbance Of MnS thin film is determined from the range 300-900 nm**.** **(**Fig 2a) shows absorbance as-deposited nanostructured MnS thin film.

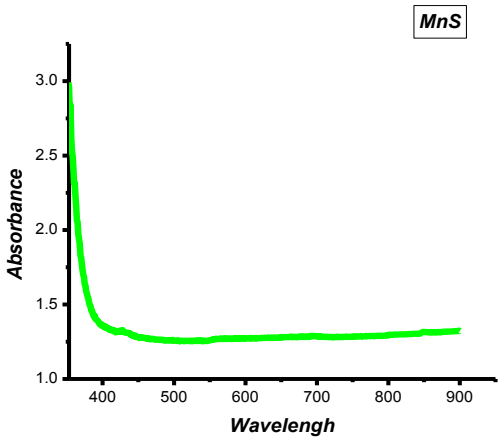

(Fig.2a) Shows absorption spectra of Nanostructured MnS thin film

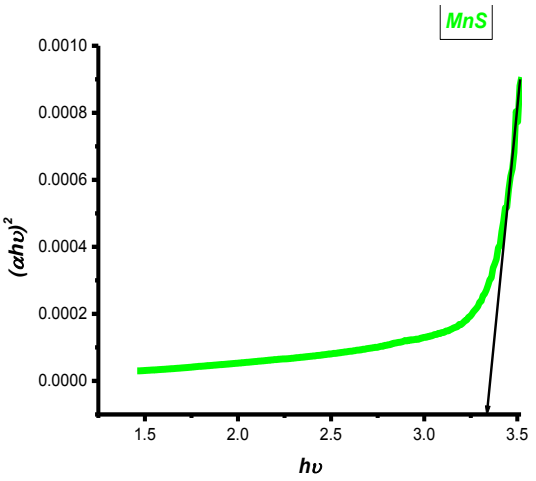

(Fig.2b) shows the band gap of nanostructured MnS thin film.

(Fig 2a) shows band gap of nanostructured MnS thin film obtained from absorption spectra **.**The band gap energy could be obtained from the plot of $(\alpha h \nu)^2$ as a function of (h ν) (Figure 2b). A sharp cut off is obtained from absorption spectra at ~380 nm which corresponds to band gap energy of 3.33 eV [21-22]. The observed value is greater than the standard band gap (3.1 eV) of MnS material, showing a `blue shift' of 0.23 eV. This is attributed to size quantization in nanocrystalline semiconductors. This size quantization occurs due to localization of electrons and holes in a confined volume of the semiconductor nanocrystallites.

3.3 Optical study of $Zn_{0.8}Mn_{0.2}S$ thin film were (x=0.2)

The optical absorbance of **$Zn_{0.8}Mn_{0.2}S$** thin film is determined from the range 300-900 nm**.** **(**Fig.3a) exhibits the UV-visible absorption spectrum of Mn^{2+}-doped ZnS thin film deposited on a glass substrate. This absorption spectrum exhibits a shoulder at 315 nm (3.93 eV), resulting from the quantum confinement effect of Mn^{2+}-doped ZnS thin film . It suggests a large blue shift of 0.26 eV of the absorption band from that of 338 nm (3.67 eV) for bulk ZnS crystals at room temperature [1,2]. Thus, the band gap of Mn^{2+}-doped ZnS nanoparticles has been enlarged.

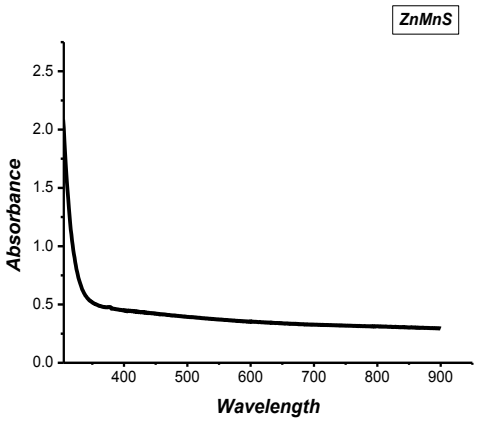

(Fig.3a) Shows absorption spectra of Nanostructured $Zn_{0.8}Mn_{0.2}S$ thin film

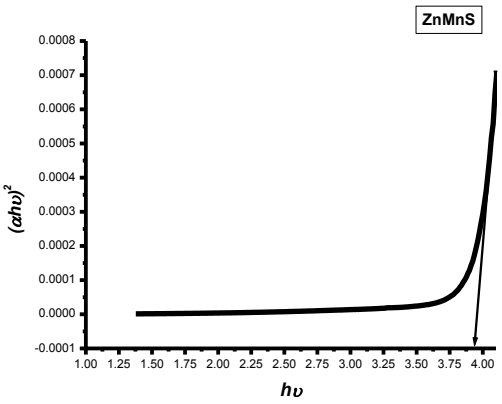

(Fig.3b) shows the band gap of nanostructured $Zn_{0.8}Mn_{0.2}S$ thin film

(Fig 3b) shows band gap of nanostructured ZnS thin film obtained from absorption spectra The band gap energy could be obtained from the plot of $(\alpha h\nu)^2$ as a function of $h\nu$ (Fig. 3b) . A sharp cut off is obtained from absorption spectra at ~315 nm which corresponds to band gap energy of 3.93eV .

3.4 Magnetic properties

(Figure 4a, b, c) show the magnetization (M) versus magnetic field (Oe) curves of $Zn_{1-x}Mn_xS$ nanocrystalline thin films at 300 K. The magnetization curves were obtained with the applied field parallel to the plane of the samples. We observe that the M (H) curves indicate paramagnetic behavior for 0 at.% Mn-doped ZnS nanocrystalline thin films. This can be concluded that the Mn ions not existed as a single impurity. However, 20 and 100 at.% Mn-doped ZnS nanocrystalline thin films exhibit a ferromagnetic behavior at 300 K which was in good agreement with other reports on Mn-doped ZnS thin films synthesized by the sol–gel spin coating technique [23] and Mn-doped zinc oxysulfide films prepared by a spray pyrolysis method [24]. Apart from these, Kanmani et al. [25] reported the antiferromagnetic with diamagnetic behavior in Mn-doped ZnS nanoparticles at room temperature and they explained the origin of observed antiferromagnetic behavior by the coupled antiferromagnetic interaction between Mn ions.

The low field dependent hysteresis loops of the $Zn_{1-x}Mn_xS$ nanocrystalline thin films are given in (Fig. 5) indicating the coercive field (Hc) values 220 Oe,260 Oe for (X= 0.2 and 1 respectively) . The saturation magnetization (Ms) values of Mn-doped ZnS nanocrystalline thin films can not be exactly determined , since they have not saturated.

However, as shown in (Fig. 5) it is obvious that the ferromagnetic signal for 100 at.% Mn-doped ZnS sample is lower than that of 20 at.% Mn-doped ZnS sample. This behavior attributed to the occurrence of antiferromagnetic coupling might increase

due to the shorter separation distances between Mn pairs with increasing Mn concentration, which leads to suppressing of the ferromagnetic interaction [26 -28]. Nevertheless, 20 at.% Mn-doped ZnS sample has the highest the ferromagnetic signal than that of other samples. It is expected that by increasing the Mn concentration in $Zn_{1-x}Mn_xS$ system, many point defects will occur and this can contribute in ferromagnetic properties of DMS [24, 29, 30]. Hence, for the highest ferromagnetic signal of 20 at.% Mn-doped ZnS, our sample might be attributed to the formation of donor–acceptor pair recombination in $Zn_{1-x}Mn_xS$ system as the dominant defect, due to incorporation of Mn into substitutional zinc site in Zn crystallites as suggested by Ragam et al. [30].

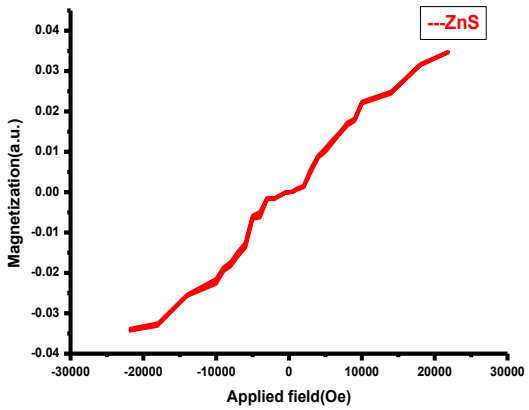

Fig. 4a Magnetic hysteresis curve of $Zn_{1-x}Mn_xS$ thin film with Mn content (x = 0.0) at 300 K

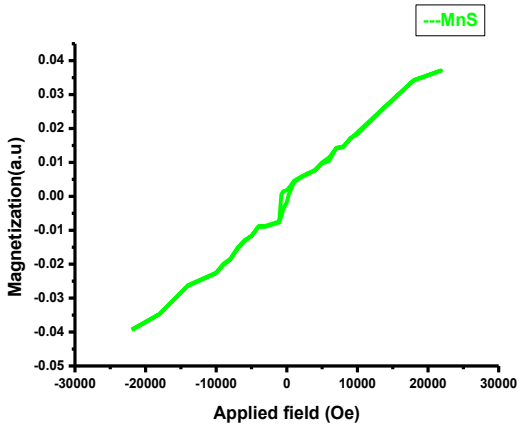

Fig. 4b Magnetic hysteresis curve of $Zn_{1-x}Mn_xS$ thin film with Mn content (x = 1.0) at 300 K

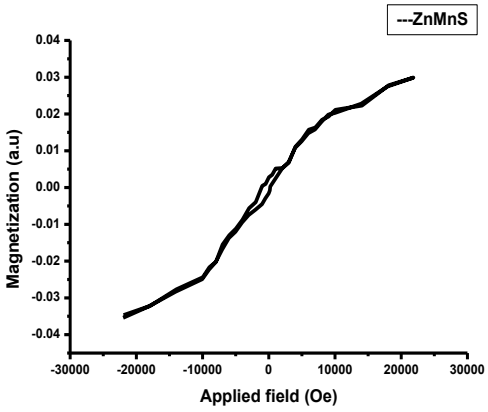

Fig. 4c Magnetic hysteresis curve of $Zn_{1-x}Mn_xS$ thin film with Mn content (x = 0.2) at 300 K

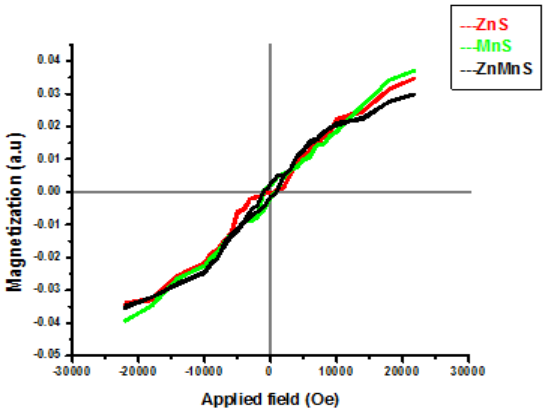

Fig. 5 Magnetic hysteresis curves of $Zn_{1-x}Mn_xS$ thin films with different Mn contents (x = 0.0, 0.2, and 1) at 300 K

In case of the Mn-doped ZnS nanoparticles no room temperature ferromagnetism was observed in the Mn-doped ZnS nanoparticles synthesized by co-precipitation method [25 , 31]. In this context, we concluded that our $Zn_{1-x}Mn_xS$ thin films are much better than the Mn-doped ZnS nanoparticles or nanocrystalline thin films, synthesized by other conventional methods.

The possible origins of the ferromagnetic behavior of the Mn-doped ZnS nanocrystalline thin films can be assessed by considering the followed reasons: (1) the intrinsic property of Mn-doped ZnS samples which can be attributed to the coexistence of ferromagnetic and antiferromagnetic interaction between the second neighbors Mn spins through indirect Mn–S–Mn exchange [32 ,33]; (2) point defects such as oxygen vacancies, zinc vacancies, zinc interstitials and sulfur vacancies that can play significant roles on ferromagnetic properties of Mn doped II–IV and III–V based semiconductors [24, 29 , 34, 35, 36]; (3) the hybridization between the transition metal atoms and S atoms plays an important role in the formation of the induced magnetic moments, the Mn atoms induce ferromagnetic behavior, suggested by Chen et al. [37]; (4) The smaller size of the synthesized nanostructures might result in the net magnetic moment produced due to non exact compensation of the two magnetic sub-lattices. This non-compensation at the surface of the ZnS nanostructures may be the cause of observed ferromagnetism. In Mn-doped nanocrystalline thin films, p-orbitals are more localized and interact more strongly with spin magnetic moments of d-orbitals of Mn ions and giving a higher net magnetization. The exact origin of magnetism is still not clear and may require additional study. Therefore, we suggested that the ferromagnetism in our Mn-doped ZnS samples might be due to the point defects specially sulfur vacancies .

5 CONCLUSIONS

Nanocrystalline $Zn_{1-x}Mn_xS$ thin films were fabricated on glass substrates chemical bath deposition technique . It was found that by increasing the Mn doping ratio the lattice parameters did not decrease and Mn ions were substituted in place of Zn ions. Band gap energy (Eg) increased from 3.70 to 3.93 eV upon Mn doping content, which may be attributed to the increase of the lattice parameter. The observed ferromagnetism might be arising from the point defects such as zinc vacancies, zinc interstitials and sulfur vacancies or indirect Mn–S–Mn exchange interaction.

ACKNOWLEDGEMENT

The one of author are thankful to the Head, department of Nanotechnology, Dr. Babasaheb Ambedkar Marathwada University, Aurangabad for providing the laboratory facility to carry out the research work.

REFERENCES

(1) J.Han, C. Spanheimer, G. Haindle, G. Fu, V. krishnakumar, J. Schaffner, C. Fan Zhao, K.Klein, W. Jaegermann, Sol Energy Mater Sol Cells **95**, 816-820, (2011).

(2) H. Neumann, W. Horig, E. Reccius, H. Sobotta, B. Schumann, G. Kuhn, Thin Solid Films **61**, 13,(1979).

(3) Tang, W.; Cameron, D. C. Thin solid Film 1996, 28

(4) Yang, H.; Holloway, P. H. J. Phys. Chem. B 2003, 107, 9705.0, 221.

(5) Leeb, J.; Gebhardt, V.; Muller, G.; Haarer, D.; Su, D.; Giersig, M

(6) Le-Xi, S.; Kuen-Huei, C.; Huey-Liang, H. Appl. Surf. Sci. 2003, 212,305.

(7) Nina, I. K.; Eugenia, V. B.; Chad, C. W.; Benjamin, R. M.; Thomas,M. Chem. Mater. 2000,12, 383.

(8) Lo´pez, M. C.; Espinos, J. P.; Martı´n, F.; Leinen, D.; Ramos-Barrado, J. R. J. Cryst. Growth 2005, 285, 66.

(9) Herna´ndez-Fenollosa, M. A.; Lo´pez, M. C.; Donderis, V.; Gonza´lez, M.; Marı´, B.; Ramos-Barrado, J. R. Thin Solid Films 2008, 516,1622.

(10) Lee, E. Y. M.; Tran, N. H.; Russell, J. J.; Lamb, R. N. J. Phys. Chem. B 2003, 107, 5208.

(11) Chun, J.; Talaga, D. S.; Zink, J. I. J. Am. Chem. Soc. 1997, 119, 163.

(12) Zhang, L.; Szargan, R.; Chasse´, T. Appl. Surf. Sci. 2004, 227, 261.

(13) Tsukasa, T.; Atsushi, O.; Susumu, K.; Hidehiro, Y.; Hirotaro, M.; Hiroshi, Y. Langmuir 2000, 16, 5820.

(14) Goudarzi, A.; Motedayen Aval, G.; Sahraei, R.; Ahmadpoor, H. Thin Solid Films 2008, 516, 4953.

(15) Oladeji, I. O.; Chow, L. Thin Solid Films 1999, 339, 148.

(16) Hubert, C.; Naghavi, N.; Canava, B.; Etcheberry, A.; Lincot, D. Thin Solid Films 2007, 515, 6032.

(17) Ben Nasr, T.; Kamoun, N.; Kanzari, M.; Bennaceur, R. Thin Solid Films 2006, 500, 4.

(18) Oladeji, I. O.; Chow, L. Thin Solid Films 2005, 474, 77.

(19) Gode, F.; Gumus, C.; Zor, M. J. Cryst. Growth 2007, 299, 136.

(20) Hubert, C.; Naghavi, N.; Etcheberry, A.; Roussel, O.; Hariskos, D.; Powalla, M.; Kerrec, O.; Lincot, D. Phys. Status Solidi A 2008, 205.

(21) N.Kamoun Allouche, T. Ben Nasr, N. Turki Kamoun, C. Guasch, Materials Chemistry and physics, **123**, 620-624,(2010).

(22) Y. Kavanagh, D. C. Cameron, Thin solid films, **398-399**, 24-28, (2001).

(23) Ni WS, Lin YJ, Liu CJ, Yang YW, Horng L (2013) J Alloy Compd 556:178–181

(24) Polat I, Aksu S, Altunbas M, Yılmaz S, Bacaksız E (2011) J Solid State Chem 184:2683–2689

(25) Kanmani SS, Rajkumar N, Ramachandran K (2011) J Nano Electron Phys 3:1064–1070

(26) Xu HY, Liu YC, Xu CS, Liu YX, Shao CL, Mu R (2006) J Chem Phys 124:074707

(27) Elanchezhiyan J, Bhuvana KP, Gopalakrishnan N, Balasubramanian T (2008) Mater Lett 62:3379–3381
(28) Chen W, Zhao LF, Wang YQ, Miao JH, Liu S, Xia ZC, Yuan SL (2005) Appl Phys Lett 87:042507
(29) Ni WS, Lin YJ, Liu CJ, Yang YW, Horng L (2013) J Alloy Compd 556:178–181
(30) Ragam M, Sankar N, Ramachandran K (2011) Defect Diffus For 318:11–21
(31) Peng WQ, Qu SC, Cong GW, Zhang XQ, Wang ZG (2005) J Cryst Growth 282:179–185
(32) Delikanli S, He S, Qin Y, Zhang P, Zeng H, Zhang H, Swihart M (2008) Appl Phys Lett 93:132501
(33) Bhattacharyya S, Estrin Y, Rich DH, Zitoun D, Koltypin Y, Gedanken A (2010) J Phys Chem C 114:22002–22011
(34) Goktas A, Mutlu IH, Yamada Y, Celik E (2013) J Alloy Compd 553:259–266
(35) Liu H, Zhang X, Li L, Wang YX, Gao KH, Li ZQ, Zheng RK, Ringer SP, Zhang B, Zhang XX (2007) Appl Phys Lett 91:072511
(36) Quynh Hoa TT, Duc The N, McVitie S, Nam NH, Van Vu L, Canh TD, Long NN (2011) Opt Mater 33:308–314
(37) Chen H, Shi DA, Qi J (2011) J Appl Phys 109:084338